Automated Measurement of Human Skeletal Calf Muscle Contraction via B-Mode Ultrasound Imaging

Ryan J. Cunningham[1]
r.cunningham@mmu.ac.uk
Peter J. Harding[2]
p.harding@mmu.ac.uk
Ian D. Loram[2]
i.loram@mmu.ac.uk
Nicholas P. Costen[1]
n.costen@mmu.ac.uk

[1] School of Computing, Mathematics and Digital Technology
Manchester Metropolitan University

[2] School of Healthcare Science,
Manchester Metropolitan University

Abstract

Traditionally surface Electromyography (EMG) has been used to non-invasively identify the activation of superficial skeletal muscle. We propose that the automated analysis of Ultrasound (US) images can provide an alternative technique by which active and passive muscle movement may be classified. We present a method by which the change in muscle shape can be extracted from pairs of sequential US images and used to classify whether that shape change was caused by active or passive muscle lengthening. Results are presented which show that our method can correctly classify active and passive movements with greater than 95% accuracy and is less affected by change in contraction strength than EMG.

1 Introduction

There are many methods available that provide ways by which muscle activity can be analysed - most notably EMG (surface) or IEMG (intramuscular). Electrodes placed on the skin (EMG) can measure activation of superficial muscle but there is an inherent level of noise which can make it difficult to identify activation at small forces/velocities; this is particularly true if a small activation co-occurs with a larger one. Filtering an EMG metric can help in the extraction of meaningful physiological information about muscle activity, but often the signal to noise ratio is too low to reveal anything at low force exertion [4]. Thin wire electrodes inserted into the muscle through the skin (IEMG) can measure contraction in both superficial and deep muscle, and is generally considered a more accurate representation of activity than EMG. IEMG is more susceptible to external electrical noise, measures a small volume within the muscle, and is invasive (IEMG requires a sterile environment; there is also an inherent risk factor when measuring motor neurons near the spine and neck). Ultrasound has been considered by many as a possible alternative method of measuring activity in

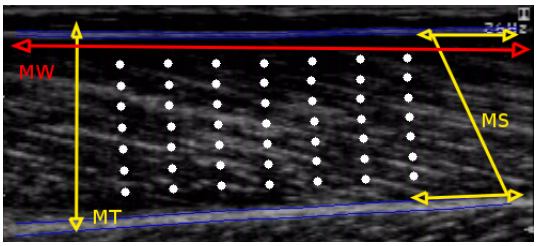

Figure 1: ASM segmented (blue contours) US of relaxed GM (Gastrocnemius Medialis; superficial muscle in the calf) and array of point features (white dots) over GM. Sheer, thickness and width (MS, MT, MW) are calculated as: the mean difference in x displacement of the top and bottom row of point features, the mean difference in y displacement of the top and bottom row of point features, and the mean difference in x displacement in the leftmost and rightmost columns.

skeletal muscle [3, 4, 5, 6]. US is entirely non-invasive, risk free, cost effective, and has been shown to be more sensitive to architectural changes (such as pennation angle, cross-sectional area) resulting from contraction than EMG at low force exertion [4, 6]. US can also analyse a much greater cross-sectional area of muscle tissue.

Recent work [3] has demonstrated that with the application of computer vision techniques (such as ASM [1], and KLT feature tracking [7, 8]), useful information about muscle architectural changes can be automatically derived from US. We propose that further to this, measures derived from architectural changes of muscle can be used to correctly identify whether the shape change was caused by external forces (i.e. passively) or by voluntary contraction (i.e. actively).

2 Methodology

2.1 Segmentation and Motion Tracking

An ASM was used to segment $25Hz$ US video sequences of GM, then KLT features were selected within the intramuscular area on a 7×7 grid arrangement and tracked into the next frame. The ASM segmentation was then updated and features re-selected to prevent tracking drift beyond the image boundary. A square KLT feature window size of $55px$ was used across all trials. Figure 1 illustrates the tracking process. GM contours in 450 images (describing range of motion for each participant) were marked up and used to train the ASM. The principal component model was constructed at runtime from the mark-up database.

A non-standard initialisation step was used with this model. At the start of each video sequence, the most accurate mean shape was chosen from all known participant shape means. This is done by iterating over each participant mean and calculating the Mahalanobis distance from each contour point to the statistical models of gradient calculated during training. At this point the best fit from the participant i.e. that with the lowest total Mahalanobis distance, was used as the "mean shape" for the duration of that video sequence. Other than this change, the ASM used was as defined in [1]. This method of segmentation and tracking is described in detail in previous work [3].

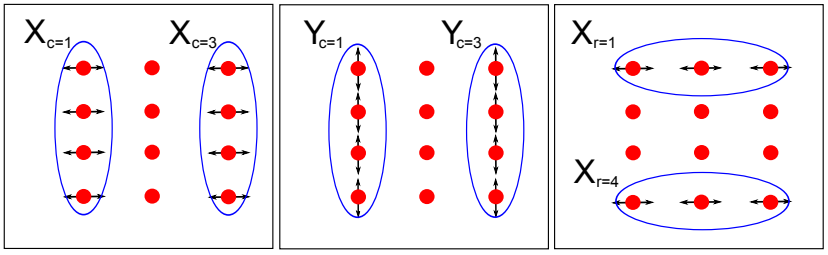

Figure 2: Left: A 3-item vector of x-direction displacements per column (sheering). Centre: A 3-item vector of y-direction displacements per column (thickening). Right: A 4-item vector of x-direction displacements per row (widening).

2.2 Muscle Shape Change Modelling

Previous measures used to assess muscle shape change have included muscle thickness and muscle sheering [4, 6], in addition to these measures muscle widening is also considered in our analysis (see Figure 1). Rather than distilling the muscle shape change between two frames into 2 or 3 scalar metrics, the use of grid sampling over the entire cross-sectional area of the muscle provides additional information about the active or passive nature of that shape change. All of the 49 point features were considered on a frame by frame basis, in the analysis. Figure 2 shows examples of how information is extracted that can be used to approximate width, thickness and sheering from the point features.

To use the entirety of the data would result in a 98-dimensional feature vector, where the sample size is 6,672. For reduction of dimensionality the mean sheering per column, $\bar{\mathrm{S}}_c$, mean thickening per column, $\bar{\mathrm{T}}_c$, and mean widening per row, $\bar{\mathrm{W}}_r$ were computed. Since the magnitude of active movement over passive movement is ≈ 1 order of magnitude greater [6], in order to avoid solving an ill-posed problem, velocity was removed from the data by normalising on a per frame basis, giving a relative velocity (shape of motion). Sheering, thickening and widening measures (SS, ST, SW) are created as

$$\begin{array}{rrrrr} \mathrm{SS} = \{ & \bar{\mathrm{S}}_c & \}\forall c = \{ & \mathrm{X}_{cr} & \}\forall r \\ \mathrm{ST} = \{ & \bar{\mathrm{T}}_c & \}\forall c = \{ & \mathrm{Y}_{cr} & \}\forall r \\ \mathrm{SW} = \{ & \bar{\mathrm{W}}_r & \}\forall r = \{ & \mathrm{X}_{cr} & \}\forall c. \end{array} \tag{1}$$

This leaves 3 vectors containing 7 mean displacement values which are uses as a 21 dimensional descriptor of shape change between each two frames.

2.3 Activity Determination

An SVM [2] was used for the classification of active and passive shape changes. The training data was labelled using force exerted in active trails per participant to define when the muscle is being moved actively, and corresponding frames of each following passive trial to define when the muscle was being moved passively. The segmentation was defined as

$$s(v,t) = \left((f_{vt} > \sigma_v) \vee \left(\frac{d(f_{kt})}{dt} > \sigma_k \right) \right) \neg \left(\frac{d(f_{kt})}{dt} < -\sigma_k \right) \tag{2}$$

where v is the trial, t is the frame, k is a constant ($k = 1$), σ_v is the standard deviation of force in trial v, and f_{vt} is the force in trial v at frame t.

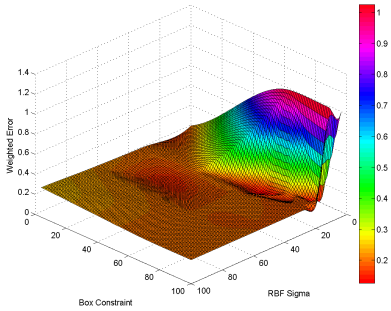

Figure 3: SVM optimisation error surface, where the cost function $\mathrm{E}(D^{-},C,\sigma)$ (see Equation 4) is plotted against RBF σ and the SVM Box Constraint, C.

Leave one participant out cross validation was used to train the SVM, where a single participant's data was used to validate and all remaining participants' data was used to train. Both the training and validation data were created from the sheer, thickness and width measures according to

$$D = \{|SS_t, ST_T, SW_t|\}\forall t. \tag{3}$$

The SVM used here had a Gaussian Radial Basis Function (RBF) kernel and was trained with the binary training signal of all participants, to differentiate between active and passive shape changes. The SVM was optimised during training by varying the hyperplane margin C and the RBF σ parameters. The optimisation function - where minimal distance between the two errors reduces the bias on the training samples - is defined as

$$\begin{aligned} \mathrm{E}(D^{-},C,\sigma) &= \frac{S_{\sigma C}(D^{-})_{error}+S_{\sigma C}(D)_{error}}{2} + |S_{\sigma C}(D^{-})_{error} - S_{\sigma C}(D)_{error}| \\ \text{Minimise} &: \mathrm{E}(D^{-},C,\sigma) \;\; \forall C \in \mathbb{R} : 0 \to e^{4.5}, \;\; \forall \sigma \in \mathbb{R} : 0 \to e^{4.5}, \;\; \forall D^{-} \in D \end{aligned} \tag{4}$$

where D^{-} is the validation set $D^{-} \in D$, D is the training set $D \in \{x_1, y_1, ...x_n, y_n\} - D^{-}$ and $S_{\sigma C}(D)_{error}$ is the error of the SVM ($S_{\sigma C}$) on the set D.

2.4 Data Collection

Simultaneous US and EMG measurements were made over 3 sets of 2 trials (20s duration) with 12 participants, positioned upright with their backs against a stiff board, standing on programmable foot pedals. For the first of each set (trial a) participants rotated the foot pedals in a plantarflexion (increasing the joint angle between shank and foot) motion (with a diminished level of force from trials 1–3), while maintaining their body posture; the pedals automatically returned to level if no force was exerted. The force exerted (Nm) and foot pedal angle (degrees) were recorded at 1000Hz. The force was used to actuate the motors on the foot pedals which caused an ankle plantarflexion rotation. For the second of each set (trial b) participants allowed their ankle angle to rotate freely with the pedals while maintaining posture; the recorded angle from each participant's trial a was used to drive the motors in

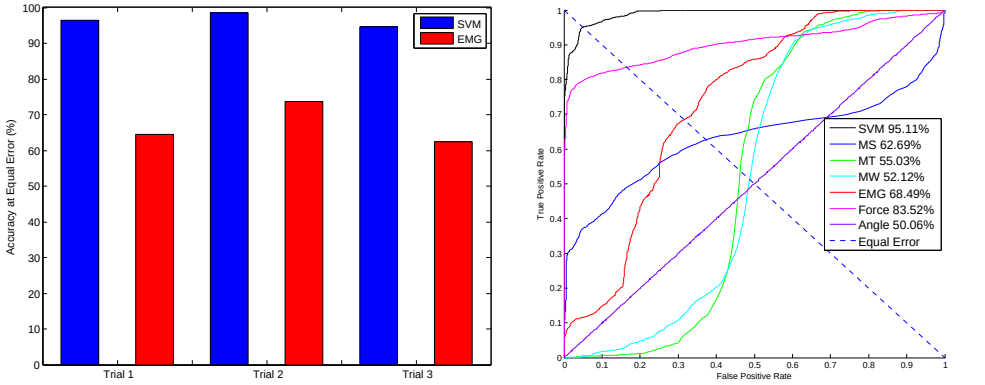

Figure 4: Left: SVM/EMG comparison showing accuracy at equal error over contraction strengths for all participants. Right: ROC curves for all participants over trials 3*a*–3*b* (lowest activity trials) only, showing accuracy at equal error.

trial *b*, resulting in passive muscle length changes occurring within the corresponding time frame to the active muscle length changes in trial *a*. Data were recorded via EMG over the GM muscle at $1000Hz$, and an US probe secured to GM. All US video sequences were collected at a static temporal resolution of $25Hz$.

2.5 Data Processing

EMG was filtered with a sixth order high pass Butterworth filter, followed by rectification and a second order, low pass filter. Cubic interpolation was used to re-sample the recorded US measures (see Equation 1) from $25Hz$–$1000Hz$. The data were realigned temporally via cross-correlation of US and external measures, with a maximum possible US realignment of 15 frames (assuming that US measures will always lag behind force output). On average US lags the external measures by ≈ 13 frames ($0.52s$).

3 Results

Receiver Operating Characteristics (ROC) (see Figure 4) were computed on the optimised, cross-validated SVM and all other measures. An ROC threshold step interval of $\frac{1}{500}$ was used. After filtering the SVM time-series output with a low pass Butterworth filter, the SVM shows a highly reliable classification accuracy of 95.11% at equal error. Independent US metrics (MS, MT, MW) report reasonable accuracy, with fascicle sheering operating at 62.69% accuracy at equal error. EMG does prove reliable in the majority of cases, but for some participants the noise threshold was enough to bring the accuracy down to 68.49% at equal error. The significance of these results is in the fact that they represent the classification accuracy of low force muscle activations. Figure 4 (Left) shows that the SVM (Ultrasound) is more accurate over all trials, than EMG, with greater consistency at lower force exertions. The average peak force exertion over all participants for trial 3*a* is $21.47Nm$, and the average peak foot pedal angle is 4.37°. The average peak force exertion over all participants for trial 1*a* is $64.35Nm$ and the average peak for foot pedal angle is 8.51°.

4 Conclusions

It has long been established that there is a non-linear relationship of sensitivity to physiological change under force between US and EMG, with US being more sensitive to change at smaller activations in the isometric case [4]. It has previously been established that these changes can be measured automatically [3, 6]. We have shown that it is possible to correctly classify an active or passive muscle shape change from automated analysis of temporal skeletal muscle US, even when the joint rotation angle is identical. The technique presented here has also been shown to offer a more accurate classification between active and passive muscle shape change than surface EMG on this data set. This method establishes a starting point in the construction of a comprehensive model of human muscle function, which combines muscle length change, activation and joint angle. Future work will explore the wider application of this technique to other, less accessible, muscles such as deep muscles near the spinal cord and cervical muscles in the neck.

References

[1] T.F. Cootes, D. Cooper, C.J. Taylor, and J. Graham. Active shape models - their training and application. *Computer Vision and Image Understanding*, 61(1):38–59, 1995.

[2] C. Cortes and V. Vapnik. Support-vector networks. *Machine Learning*, 20(3):273–297, 1995.

[3] J. Darby, E.F. Tole, N.P. Costen, and I.D. Loram. Automated regional analysis of b-mode ultrasound images of skeletal muscle movement. *Applied Physiology*, 112(2):313–327, 2012.

[4] P.W Hodges. Measurement of muscle contraction with ultrasound imaging. *Physical Therapy*, 13(4):18–28, 2003.

[5] I.D. Loram, C.N. Maganaris, and M. Lakie. Use of ultrasound to make noninvasive in vivo measurement of continuous changes in human muscle contractile length. *Applied Physiology*, 100(4):1311–1323, 2006.

[6] I.D. Loram, I. Di Guilio, and C.N. Maganaris. The consequences of shortrange stiffness and fluctuating muscle activity for proprioception of postural joint rotations - the relevance to human standing. *Neurophysiology*, 102:460–474, 2009.

[7] J. Shi and C. Tomasi. Good features to track. In *IEEE Conference on Computer Vision and Pattern Recognition*, pages 1063–1069, 1994.

[8] C. Tomasi and T. Kanade. Detection and tracking of point features. *Pattern Recognition*, 37:165–168, 1991.